Since January 2020 Elsevier has created a COVID-19 resource centre with free information in English and Mandarin on the novel coronavirus COVID-19. The COVID-19 resource centre is hosted on Elsevier Connect, the company's public news and information website.

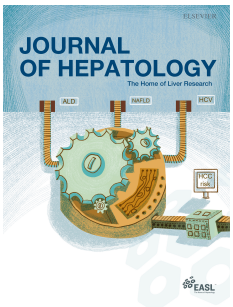

Morphologic and molecular analysis of liver injury after SARS-CoV-2 vaccination reveals distinct characteristics

Sarp Uzun, Carl Zinner, Amke C. Beenen, Ilaria Alborelli, Ewelina M. Bartoszek, Jason Yeung, Byron Calgua, Matthias Reinscheid, Peter Bonsert, Anna K. Stalder, Jasmine Haslbauer, Jürg Vosbeck, Luca Mazzucchelli, Tobias Hoffmann, Luigi M. Terracciano, Gregor Hutter, Michael Manz, Isabelle Panne, Tobias Böttler, Maike Hofmann, Bertram Bengsch, Markus H. Heim, Christine Bernsmeier, Sizun Jiang, Alexandar Tzankov, Benedetta Terziroli Beretta-Piccoli, Matthias S. Matter

PII: S0168-8278(23)00348-3

DOI: https://doi.org/10.1016/j.jhep.2023.05.020

Reference: JHEPAT 9183

To appear in: *Journal of Hepatology*

Received Date: 17 August 2022

Revised Date: 10 May 2023

Accepted Date: 19 May 2023

Please cite this article as: Uzun S, Zinner C, Beenen AC, Alborelli I, Bartoszek EM, Yeung J, Calgua B, Reinscheid M, Bonsert P, Stalder AK, Haslbauer J, Vosbeck J, Mazzucchelli L, Hoffmann T, Terracciano LM, Hutter G, Manz M, Panne I, Böttler T, Hofmann M, Bengsch B, Heim MH, Bernsmeier C, Jiang S, Tzankov A, Beretta-Piccoli BT, Matter MS, Morphologic and molecular analysis of liver injury after SARS-CoV-2 vaccination reveals distinct characteristics, *Journal of Hepatology* (2023), doi: https://doi.org/10.1016/j.jhep.2023.05.020.

SARS-CoV-2 Vaccine-Induced Liver Injury vs. Autoimmune Hepatitis

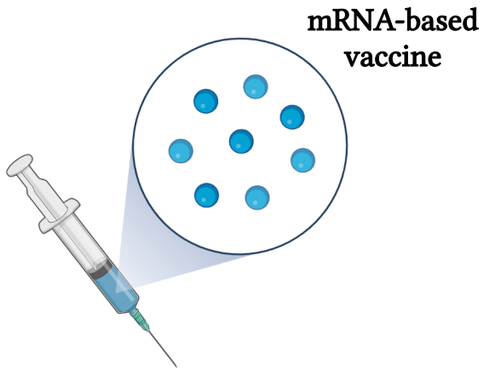

Vaccine Induced Liver Injury (VILI) n=6

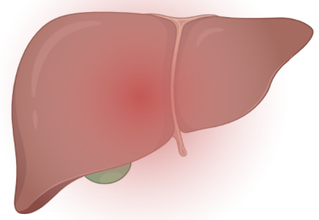

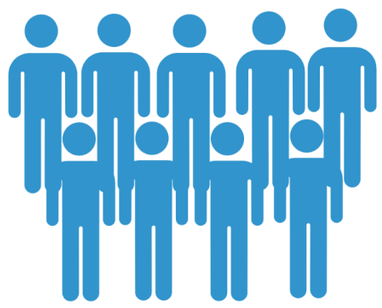

Autoimmune Hepatitis (AIH) n=9

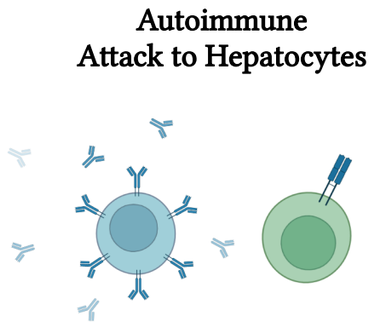

Whole & Spatial Transcriptome Sequencing

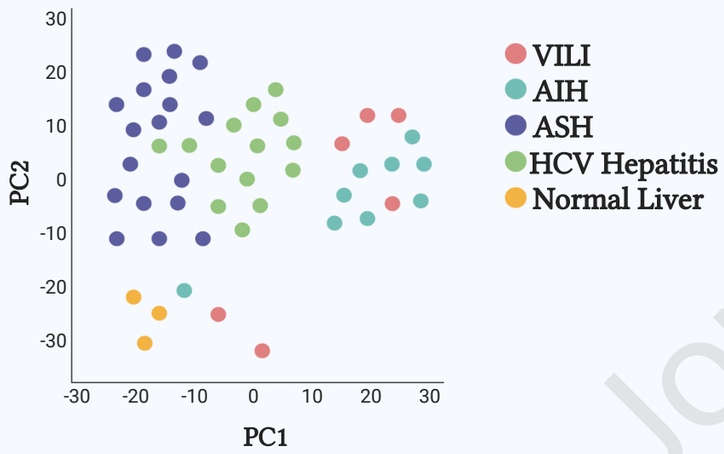

Metabolic Pathway Enrichment

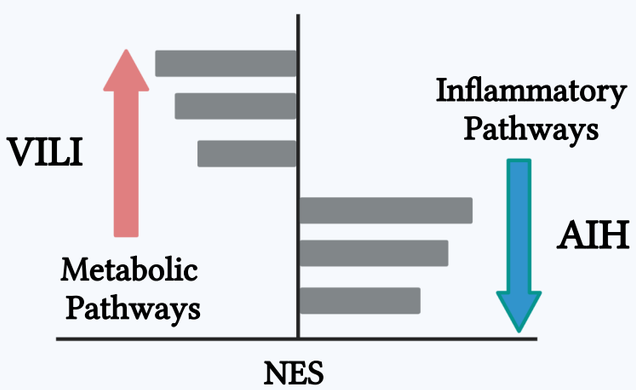

Multiplex Immunofluoresence CODEX

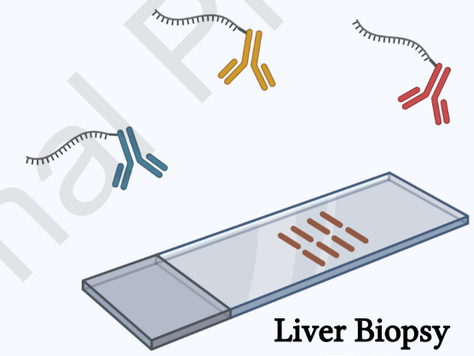

CD8 T-cell Dominant Response

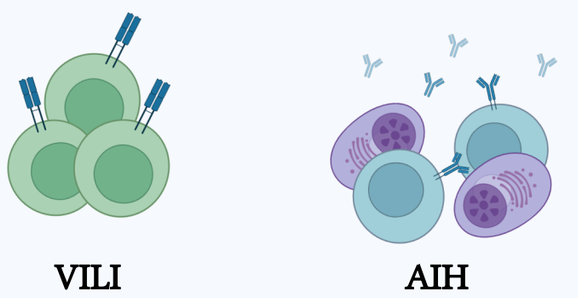

TCR & BCR Sequencing

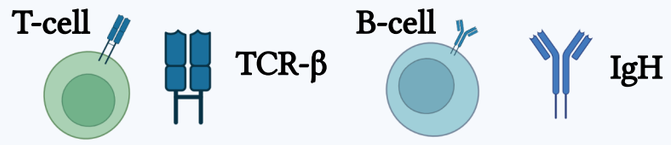

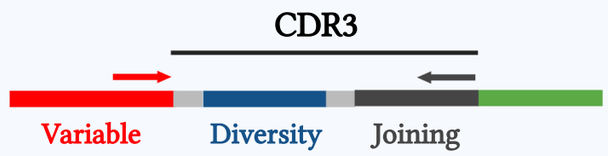

Oligoclonal Immune Repertoire

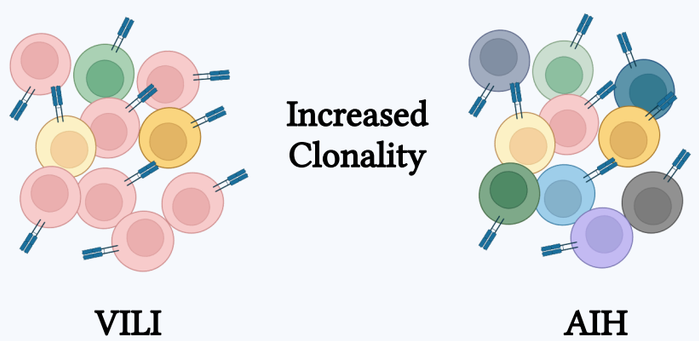

Morphologic and molecular analysis of liver injury after SARS-CoV-2 vaccination reveals distinct characteristics

Sarp Uzun[1], Carl Zinner[1], Amke C. Beenen[1], Ilaria Alborelli[1], Ewelina M. Bartoszek[2], Jason Yeung[3,4,5], Byron Calgua[1], Matthias Reinscheid[6,7], Peter Bonsert[8,9], Anna K Stalder[1], Jasmine Haslbauer[1], Jürg Vosbeck[1], Luca Mazzucchelli[10], Tobias Hoffmann[11], Luigi M. Terracciano[1,12,13], Gregor Hutter[14,15], Michael Manz[16], Isabelle Panne[16], Tobias Böttler[6], Maike Hofmann[6], Bertram Bengsch[6,17,18], Markus H. Heim[19], Christine Bernsmeier[19], Sizun Jiang[3,4,5], Alexandar Tzankov[1], Benedetta Terziroli Beretta-Piccoli[20] and Matthias S. Matter[1]

1. Institute of Medical Genetics and Pathology, Pathology, University Hospital of Basel, Basel, Switzerland

2. Microscopy Core Facility, Department of Biomedicine, University of Basel, Switzerland

3. Center for Virology and Vaccine Research, Beth Israel Deaconess Medical Center, Boston, MA, USA

4. Department of Pathology, Dana Farber Cancer Institute, Boston, MA, USA

5. Broad Institute of Harvard and MIT, Cambridge, MA, USA

6. Department of Medicine II (Gastroenterology, Hepatology, Endocrinology and Infectious Diseases), Freiburg University Medical Center, Faculty of Medicine, University of Freiburg, Freiburg, Germany

7. Faculty of Biology, University of Freiburg, Freiburg, Germany.

8. Institute for Surgical Pathology, Freiburg University Medical Center, University of Freiburg, Freiburg, Germany

9. Core Facility for Histopathology and Digital Pathology, Medical Center, University of Freiburg, Faculty of Medicine, University of Freiburg, Freiburg, Germany.

10. Istituto Cantonale di Patologia, 6600 Locarno, Switzerland

11. Innere Medizin, Spital Dornach, Spitalweg 11, 4143 Dornach, Switzerland

12. Department of Biomedical Sciences, Humanitas University, Via Rita Levi Montalcini 4, 20090 Pieve Emanuele, Milan, Italy

13. IRCCS Humanitas Research Hospital, Via Manzoni 56, 20089 Rozzano, Milan, Italy

14. Brain Tumor Immunotherapy Lab, Department of Biomedicine, University of Basel, Basel, Switzerland

15. Department of Neurosurgery, University Hospital Basel, Basel, Switzerland

16. Department of Gastroenterology, Clarunis-University Center for Gastrointestinal and Liver Diseases, St. Clara Hospital and University Hospital Basel, Postfach, 4002, Basel, Switzerland

17. Signalling Research Centres BIOSS and CIBSS, University of Freiburg, Freiburg, Germany.

18. Partner Site Freiburg, German Cancer Consortium (DKTK), Heidelberg, Germany

19. Department of Biomedicine, University of Basel, Switzerland; Clarunis, University Centre for Gastrointestinal and Liver Diseases, Basel, Switzerland.

20. Faculty of Biomedical Sciences, Università Della Svizzera Italiana, 6900, Lugano, Switzerland. Epatocentro Ticino, Via Soldino 5, 6900, Lugano

Corresponding Author: Matthias Matter, PD Dr. med. et Dr. phil. nat.

Institute of Medical Genetics and Pathology

University Hospital of Basel, Basel, Switzerland

E-mail: matthias.matter@usb.ch

Phone: +41 61 328 71 64

ORCID: 0000-0002-2005-5266

Keywords: Autoimmune hepatitis, COVID-19, Drug Induced Liver Injury, SARS-CoV-2, vaccination

Word Count: including reference: 6666 / **excluding reference:** 5534

Number of Figures and Tables: 5

Conflicts of interest

M.S.M. has served as a consultant for ThermoFisher, Merck, GlaxoSmithKline, Janssen-Cilag, Roche, Novartis and received speaker's honorary from Incyte Biosciences. G.H is cofounder of Incephalo, not related to this project. Otherwise, the authors have no conflicts of interest to declare.

Funding Sources

This study was funded by the Botnar Research Centre for Child Health (FTC-2020-10) to AT, MSM, and GH. and the Swiss National Science Foundation (SNSF; Grant No. 320030_189275) to MSM. S.J. is supported by NIH DP2AI171139, and the Bill & Melinda Gates Foundation INV-002704. The sponsor of the study did not have any role in the study design, or collection, analysis, and interpretation of data.

Author contribution

Conceptualization: SU and MSM, Methodology: SU, MSM, AB, EMB, SJ, CZ. Clinical data and patient integration: SU, MSM, JH, JV, LM, MM, IP, TH, LT, AT, MH, CB, BTBP. Sample handling and processing: SU, AB, CZ, IA, EMB, MM, IP, BCL, MR, PB, AKS, JH, JV, LM, TH, LT, AT, TB, MH, BB, MH, CB, BTBP, MSM. Software: SU, AB, CZ, IA, EMB Formal analysis: SU, AB, CZ, JY, IA, EMB, AKS, JH, JV, LM, TH, LT, AT, MH, SJ, CB, BBP, MSM. Investigation: SU, AB, CZ, IA, EMB, JY, SJ, MSM. Resources: AT, MSM. Writing - original draft: SU, MSM. Writing - review and editing: All authors. Supervision: SU, MSM. Project administration: AKS, AT, MSM. Funding: acquisition: AT, MSM, GH, SJ.

Statement of Ethics

The study was approved by the ethics commission of Northern Switzerland (EKNZ; study ID: 2020-00969), the ethics commission at the Albert-Ludwigs-University, Germany and the Comitato Etico cantonale Ticino, Switzerland. All tissue samples were collected as part of the routine diagnostic workup and selected retrospectively, informed consent was obtained from all vaccinated patients, and the study was conducted according to the Declaration of Helsinki (1975).

Data Availability Statement

The data of this study is available in Gene Expression Omnibus (https://www.ncbi.nlm.nih.gov/geo/) under GEO accession number GSE229459.

ABSTRACT

Background and Aims: Liver injury after COVID-19 vaccination is very rare and shows clinical and histomorphological similarities with autoimmune hepatitis (AIH). Little is known about the pathophysiology of COVID-19 vaccine-induced liver injury (VILI) and its relationship to AIH. Therefore, we compared VILI with AIH.

Methods: Formalin-fixed and paraffin-embedded liver biopsy samples from patients with VILI (n=6) and from patients with an initial diagnosis of AIH (n=9) were included. Both cohorts were compared by histomorphological evaluation, whole-transcriptome and spatial transcriptome sequencing, multiplex immunofluorescence and immune repertoire sequencing.

Results: Histomorphology was similar in both cohorts but showed more pronounced centrilobular necrosis in VILI. Gene expression profiling showed that mitochondrial metabolism and oxidative stress-related pathways were more and interferon response pathways less enriched in VILI. Multiplex analysis revealed that inflammation in VILI was dominated by $CD8^+$ effector T cells, similar to drug-induced autoimmune like hepatitis (DI-AILH). In contrast, AIH showed a dominance of $CD4^+$ effector T cells and $CD79a^+$ B and plasma cells. T-cell receptor (TCR) and B-cell receptor (BCR) sequencing showed that T- and B-cell clones were more dominant in VILI than in AIH. In addition, many T-cell clones detected in the liver were also found in the blood. Interestingly, analysis of TCR beta chain and Ig heavy chain variable-joining gene usage further showed that TRBV6-1, TRBV5-1, TRBV7-6 and IgHV1-24 genes are used differently in VILI than in AIH.

Conclusions: Our analyses support that SARS-CoV-2 vaccination-induced liver injury is related to AIH but also shows distinct differences from AIH in histomorphology,

pathway activation, cellular immune infiltrates, and TCR usage. VILI may be a separate entity, which is distinct from AIH and more closely related to DI-AILH.

IMPACT AND IMPLICATIONS

Little is known about the pathophysiology of COVID-19 vaccine-induced liver injury. Our analysis shows that COVID-19 vaccine-induced liver injury shares some similarities with autoimmune hepatitis, but also has distinct differences such as increased activation of metabolic pathways, a more prominent CD8+ T cell infiltrate, and an oligoclonal T and B cell response. Our findings suggest that vaccine-induced liver injury is a distinct disease entity. Therefore, there is a good chance that many patients with COVID-19 vaccine-induced liver injury will recover completely and do not develop long-term autoimmune hepatitis.

INTRODUCTION

Severe acute respiratory syndrome coronavirus 2 (SARS-CoV-2), the causative agent of coronavirus disease 2019 (COVID-19), has infected millions of people worldwide with a great socio-economic impact.[1] The most effective strategy to reduce morbidity and mortality from SARS-CoV-2 infection is the development of safe and effective vaccines. Several different COVID-19 vaccines have been approved and millions of people have received a dose to date.[2] Since the introduction of COVID-19 vaccines, potential adverse events have been reported. Most of them are mild and include local symptoms, fatigue, fever, headache, and myalgia.[2] Rarely, COVID-19 vaccination has been associated with autoimmune disorders such as myocarditis, immune thrombocytic thrombocytopenia, and Guillain-Barré syndrome.[2] In addition, several recent reports have described hepatitis following COVID-19 vaccination as a very rare event and supported a direct correlation.[3-11] Multiple potential mechanisms of COVID-19 vaccine-related tissue injury have been suggested, including molecular mimicry, triggering of a latent autoimmune disease, vaccine-induced specific antibody production, bystander activation with polyclonal B-cell expansion, epitope spreading, and the effects of particular adjuvants.[2, 12-14]

COVID-19 vaccine-induced liver injury (VILI) resembles autoimmune hepatitis (AIH) clinically, biochemically, morphologically and, to some extent, also serologically.[10, 11, 15] Many, but not all, patients with VILI fulfil the criteria for the diagnosis of autoimmune hepatitis.[10, 11, 16, 17] However, it is not known whether hepatitis following COVID-19 vaccination is a form of triggered AIH or whether it rather belongs to a condition described as drug-induced autoimmune like hepatitis (DI-AILH).[18, 19] Furthermore, very little is known about the pathophysiology of this phenomenon.[20]

In this study, we aimed to characterize the morphological and molecular features of VILI and compare them to patients with AIH. By using gene expression profiling, immune repertoire sequencing, and multiplex immunofluorescence we show that both entities share some features but also have distinct differences.

MATERIALS & METHODS

Materials and methods can be found in the supplementary documents.

RESULTS

Characteristics of study and control cohort

In our study, we included FFPE liver biopsies from six patients with COVID-19 vaccination induced liver injury (VILI) (**Table 1, Supplementary Table 1 and 2**). All patients received mRNA-1273 from Moderna, the vaccine most commonly administered in Switzerland. Two patients have been described in previous publications.[6, 11] Average patient age was 58 (range 21-85 years). Two patients were females and four were males. Three patients developed symptoms after the first vaccination and three after the second. The main symptoms were fatigue, jaundice, and nausea. The time to symptom onset varied from 2 to 28 days after vaccination. Patients did not have autoimmune diseases, except for one patient (VILI3), who had a history of elevated antibodies against thyroid peroxidase (TPO) and polymyalgia. All patients were negative by PCR or antibody testing for viral hepatitis (Hepatitis A, B, C, D, and E) and none of the patients had a history of clinically apparent COVID-19 disease. At the time of vaccination, two patients were taking several medications for concomitant diseases for more than five years (VILI5: aspirin, rosuvastatin, metformin; VILI6: lercanidipine, telmisartan). One patient had been taking oral contraceptives for three years and took herbal medicines for a short time a few months before vaccination. One patient regularly took multivitamin supplements. The remaining two patients have not taken any medicine. None of the patients had any prior history of

liver disease or alcohol abuse. After the liver biopsy, four patients received prednisone. Two patients did not receive any treatment. All patients improved and remained in remission during the follow-up period (Table 1).

Because VILI resembles AIH,[10, 11] we selected archived FFPE liver biopsies from untreated Type 1 AIH patients (n=9) for comparison, which were taken at the time of initial diagnosis of AIH and early after appearance of symptoms. AIH patients had an average age of 61 years (range 49-78 years) and were predominantly female (n=8).

Clinical and histological comparison

Serum liver enzyme levels (AST, ALT, GGT, ALP, and bilirubin) were increased in both cohorts. In comparison to AIH patients, VILI showed higher levels of AST, ALT, and bilirubin, but lower levels of GGT and ALP, without reaching statistical significance (**Supplementary Table 1 and 2**). Liver injury calculated with the R ratio[21] was hepatocellular in all VILI and AIH patients, except for one AIH patient, who had mixed, hepatocellular and cholestatic liver injury. Serum autoantibodies in the VILI cohort showed anti-nuclear antibodies (ANA) in three cases, of whom one additionally showed atypical anti-mitochondrial antibodies (AMA); one patient showed elevated anti-actin antibodies (AAA) only (**Supplementary Table 1 and 2**). Therefore, 4 out of 6 (67%) VILI patients were ANA and/or anti-smooth muscle antibodies (ASMA)/AAA positive. In the AIH cohort, 7 patients were ANA positive, two of them in conjunction with elevated ASMA or AAA. Two additional patients had either elevated ASMA or AAA only. Therefore, all patients from the AIH cohort showed elevated ANA and/or elevated ASMA/AAA. Anti-SLA, anti-LKM1, and anti-LC1 were negative in all patients from both cohorts. Two AIH patients also showed anti-neutrophil cytoplasmic antibody

(ANCA). IgG levels were increased in two out of the five tested VILI patients, and in four out of eight tested AIH patients.

After the appearance of symptoms (2 to 90 days for VILI; 9 to 150 days for AIH), all patients underwent liver biopsy and histological analysis according to current recommendations.[22-24] Variable degrees of piecemeal necrosis, confluent necrosis, focal lytic necrosis/apoptosis/inflammation, and portal inflammation were found without significant differences between the two cohorts (**Supplementary Table 1 and 3, Supplementary Figure 1)**. In contrast, confluent necrosis was more extensive in VILI (p=0.0025). The summarized Ishak grading score[24] was similar in both cohorts and between 3 and 16 (average 12.2) in patients with VILI and 6 to 14 (average 10.2) in patients with AIH. In all VILI patients and five AIH patients no fibrosis was found, corresponding to Ishak stage 0. Four AIH patients presented with stage 1 fibrosis. Rosette formation, emperipolesis, endothelialitis, and cholestasis were frequently found in both cohorts.[22, 23] Bile duct injury was present in only one patient of the VILI cohort and two patients of the AIH cohort. None of the patients showed steatosis. Likewise, there was no difference in the number of eosinophils between both cohorts.

In summary, histological analysis revealed a diagnosis of likely AIH in five out of six VILI patients and a diagnosis of possible AIH in one patient according to the most recent recommendations.[23] Moreover, 3 out of 5 VILI patients had a probable/definite AIH score according to the simplified AIH criteria (**Supplementary Table 1**).[17] For one VILI patient, not all values were available for calculation. In contrast, all AIH patients showed histologically the diagnosis of a likely AIH and a probable/definite AIH score according to the simplified criteria.

VILI and AIH patients have related but clearly different gene expression profiles

To understand the different biological mechanisms between VILI and AIH, we performed whole transcriptome profiling with bulk RNA, isolated from FFPE liver biopsies of VILI and AIH patients. As further controls, we added liver biopsies from patients with alcoholic steatohepatitis (ASH; n=17) and chronic HCV infection (n=13). HCV patients were untreated and showed high viral load at the time of biopsy. The average patient age was 64.3 years for ASH and 58.3 years for HCV patients, and both cohorts had cirrhotic liver disease (**Supplementary Table 4**). Additionally, we included three patients with histologically normal liver tissue, who presented with a metastasis to the liver (two with pancreatic and one with urothelial carcinoma). (**Supplementary Table 4**).

Principal-component analysis showed that VILI and AIH patients had different transcriptome profiles but were close to each other and significantly different from patients with chronic HCV infection or ASH (**Figure 1A**). Two patients with VILI (#1 and #2) and one patient with AIH (#7) clustered close to normal liver samples. Interestingly, all of these three patients had little inflammation signature according to RNA transcriptome (see **Figure 2A** below). Differential gene expression analysis revealed 70 genes (43 upregulated and 27 downregulated) that showed a significant difference between the VILI and AIH cohort (*lfc > 0.58*, p_{adj} *<0.05*) (**Figure 1B and Supplementary Table 5**). To validate our gene expression profiling data, we selected one significantly up- and one significantly down-regulated gene and performed a qPCR. As an up-regulated gene we selected *TSPAN8 (lfc= 2.172,* p_{adj}*=0.002)*, which has been shown to correlate with SARS-CoV-2 infection rate[25], and *RNF213 (lfc=-0.793,* p_{adj}*=0.026),* associated with immune response and interferon signaling.[26]

Expression changes were confirmed by qPCR for both genes (**Figure 1C**). Unsupervised hierarchical clustering of VILI and AIH samples based on the differentially expressed genes further showed that samples belonging to the same cohort clustered together (**Figure 1D**). Finally, we performed gene set enrichment analysis (GSEA) to identify biological processes characteristic of the VILI and AIH cohort (**Figure 1E, Supplementary Table 6**). We found that pathways related to immune response were overrepresented in the AIH cohort, in particular gene sets associated with interferon response (e.g. Hallmark Interferon-Gamma Response, Reactome Interferon Gamma Signaling, and Hallmark Interferon Alpha Response). In contrast, mitochondrial metabolism and oxidative stress-related pathways were overrepresented in the VILI cohort. Because we performed transcriptome analysis from bulk RNA, we could not determine the cell type responsible for the observed differences. However, it is known that drug-induced liver injury (DILI) results from mitochondrial toxicity and impairment of the oxidation-phosphorylation machinery in hepatocytes.[27, 28] Therefore, we carried out spatial whole transcriptome analysis with the GeoMx platform selecting arginase positive hepatocytes from periportal and centrilobular regions of VILI and AIH (**Supplementary Figure 2A and 2B**). We found 53 genes (38 upregulated and 15 downregulated) demonstrating a significant differential expression between the two cohorts (lfc > 0.58, padj <0.05) (**Supplementary Figure 2C**, **Supplementary Table 7**). GSEA revealed that the same four oxidative phosphorylation or liver metabolism related gene sets, which were enriched in bulk-RNA sequencing, were also significantly enriched with the spatial transcriptomic analysis of hepatocytes (**Supplementary Figure 2D**, **Supplementary Table 8**). Therefore, hepatocytes are the main cells responsible for the differences

between both cohorts in mitochondrial toxicity and impairment of the oxidation-phosphorylation machinery.

In summary, our data suggest that although VILI and AIH are related based on their expression profiles, they have distinct differences in biological processes.

Immunoprofiling shows higher portal/periportal CD8$^+$ T cell infiltration but lower B cell infiltration in VILI

Next, we characterized the immune infiltrates in the biopsy tissue. First, we performed a cell type enrichment analysis with our RNA gene expression data by using the xCell web tool.[29] Interestingly, we observed a more enriched “B-cells” signature in AIH patients in comparison with VILI patients (p=0.0048); however, it did not reach significance after adjustment to multiple testing (p_{adj}=0.1150) (**Figure 2A**). In contrast to B cells, no enrichment difference was observed between the two cohorts for the other immune cell signatures.

Thereafter, we carried out multiplex immunofluorescence with co-detection by indEXing (CODEX)[30] on FFPE liver biopsies of our cohorts with sufficient remaining tissue, resulting in the analysis of five VILI and seven AIH patients. By using different immune markers simultaneously (**Supplementary Figure 3A**), we assessed the density and differential localization of B and T cells within the portal and centrilobular region of the liver parenchyma (**Figure 2B, Supplementary Figure 3B**). CD79a was used as a marker for B cells including plasma cells, CD20 for B cells, CD3, CD8, CD4, and FoxP3 for respective T effector and regulatory T cells. CD3 positive T cells showed overall the highest cell density and were slightly more prominent in the portal region than in the centrilobular region in both cohorts (**Figure 2C, Supplementary Figure**

3C). $CD3^+$ $CD8^+$ T effector cells showed a trend for a higher density in VILI than in AIH in the portal (1264 vs. 734 cells/mm^2) and centrilobular region (1288 vs. 739 cells/mm^2), which did not reach significance (**Figure 2D**). $CD3^+$ $CD4^+$ $FoxP3^-$ T effector cell density was similar between VILI and AIH in the portal (897 vs. 917 cells/mm^2) and centrilobular region (265 vs.170 cells/mm^2, **Figure 2D**). Variability in immune cell density between patients within each cohort was high (**Supplementary Figure 3C and 2D**), which was already appreciated from the Ishak grading and whole transcriptome analysis described above. Therefore, we calculated the ratio between $CD3^+$ $CD8^+$ and $CD3^+$ $CD4^+$ effector T cells. Interestingly, the proportion of $CD3^+$ $CD8^+$ effector T cells in VILI was significantly higher than in AIH patients (1.541 vs. 0.7706; p=0.0303; **Figure 2E**), indicating that the immune infiltrate in VILI was dominated by $CD3^+$ $CD8^+$ T cells.

Next, we analyzed $CD3^+$ $CD4^+$ $FoxP3^+$ Treg cell distribution, which was similar in both cohorts (**Figure 2F)**. Finally, $CD20^+$ and $CD79a^+$ B cells both showed a lower density in VILI than in AIH in the portal region (CD20: 350.7 vs. 929.3 cells/mm^2; $CD79a^+$: 459.5 vs. 1267 cells/mm^2), which reached significance for $CD79a^+$ B cells (p=0.0480) (**Figure 2G)**. In the centrilobular region, $CD20^+$ B cells were similar between both cohorts, but $CD79a^+$ B cells also showed a lower density in VILI than in AIH. Interestingly, we also observed a trend towards a positive correlation between portal $CD79a^+$ B cell density and serum IgG levels in VILI and AIH cases; however, it did not reach statistical significance (r_s=0.639, p=0.052) (**Supplementary Figure 3E**).

In conclusion, inflammation in VILI was dominated by $CD8^+$ effector T cells, whereas AIH showed a significantly higher portal infiltrate of $CD79a^+$ B cells and plasma cells. Indeed, the ratio of $CD3^+$ $CD8^+$ T effector cells to $CD79a^+$ B cells was significantly higher in VILI than in AIH (**Figure 2H**). The total density of T and B cells

also correlated with Ishak grading (r_s=0.749, p=0.006) which indicated that our histopathological observations are in line with multiplex immunofluorescence analysis (**Figure 2I**). In addition, we compared a small cohort (n = 4) of DI-AILH with VILI and AIH. Liver histology, serology and clinical characteristics of DI-AILH patients showed similarities with AIH (**Supplementary Table 9 and 10**). Two patients had a definite and two a probable AIH score according to the simplified AIH criteria.[17] Interestingly, the proportion of $CD3^+$ $CD8^+$ to $CD3^+$ $CD4^+$ effector T cells and $CD3^+$ $CD8^+$ to $CD79a^+$ B cells was higher in DI-AILH than in AIH patients (1.255 vs. 0.7706 and 6.316 vs. 0.6023) (**Supplementary Figure 4**), indicating that the composition of the immune infiltrate in DI-AILH is similar to VILI but different from AIH.

VILI cohort shows less evenness in TCR and BCR repertoire and larger clonal space of top 1% T cell clones

As a next step, we characterized the clonal distribution of the adaptive immune infiltrate in VILI and AIH patients. We performed NGS-based immunoprofiling by sequencing the CDR3 region of the TCR and BCR from bulk RNA isolated from liver biopsies. After applying stringent quality criteria, we obtained valid NGS data from all samples for BCR analysis (n=15), whereas TCR analysis was carried out with six samples from each cohort (n=12).

First, we started with the analysis of global immune repertoire metrics to assess clone number, diversity, and clonality as parameters for immunological complexity and for ongoing, successful, or deregulated immune response. Although VILI had increased T and B cell clone numbers, we did not find a significant difference between both cohorts (**Figure 3A, B**). Moreover, the Shannon diversity index of both cohorts

was similar in TCR and BCR repertoires. However, we found that VILI had significantly lower evenness in TCR (p=0.0212) and BCR repertoire (p=0.0008), which indicated that VILI had more expanded clones in T and B cell architecture in comparison to AIH (**Figure 3A, B**). Indeed, the spectratyping plots of T- and B-cell clone distribution in VILI samples showed few expanded T and B cell clones, suggesting a clonal expansion against specific antigens (**Supplementary Figure 5A, B**). In contrast, the clonal distribution of T and B cells was mainly composed of unexpanded clones in AIH samples, which suggested a more polyclonal reaction against antigenic stimulations (**Supplementary Figure 5A, B**). Next, we tested whether the evenness difference between the two cohorts arises specifically from the most abundant T cell and B cell clones in the liver tissues. For this purpose, we performed clonal space analysis that was previously used to determine which ranges of clones are associated with the TCR repertoire difference.[32, 33] First, T and B cell clones were divided into four groups according to their ranked frequencies (top 1%, top 1-2%, top 2-5%, and >5%). Thereafter, the clone frequency in each group in relation to the total immune repertoire was calculated. As expected from the difference in evenness, we found that the T cell clones in the top 1% group of the VILI cohort had a significantly larger clonal space compared to the AIH cohort (27.9% vs. 16.8%; p=0.0104; **Figure 3C**). This suggests that this group of T cells is the main responder against vaccination-related antigenic stimulation. In contrast, there was no difference in the top 1-2% and top 2-5%. Since the T cell architecture was dominated by the top 1% in VILI samples, the >5% group occupied a larger space in AIH compared to the VILI cohort, however, it did not reach significance (mean VILI vs. AIH: 54.0% vs. 65.1%, p=0.0754). We also tested whether the total frequency of top 1% T cell clones correlated with the evenness in each patient and found that these two parameters showed a significant inverse correlation with

each other (r_s = - 0.797, p=0.0029; **Figure 3D**). In the B cell compartment, the top 1%, top 1-2%, and top 2-5% had a significantly larger clonal space in the VILI cohort, whereas the >5% group occupied a larger space in AIH than in VILI (**Figure 3E**). This highlights the more pronounced presence of a general B cell clone expansion in VILI samples and is consistent with the difference in evenness between VILI and AIH samples (**Figure 3E**).

Next, we analyzed in more detail the sharing of T-cell clone sequences and their specificity. Of the 184 top 1% T-cell clones among all six VILI liver samples, no shared clones were detected among them. Yet, when we uploaded the beta chain CDR3 sequences of the 184 top 1% liver T-cell clones to a publicly available TCR database (http://tools.iedb.org/tcrmatch/), we found seven spike SARS-CoV-2 glycoprotein epitopes that matched with CDR3 sequences (**Supplementary Table 11**), indicating that some high-frequency T-cell clones may possibly recognize the spike glycoprotein. From one patient (VILI #5), blood sample was available from the time of liver biopsy. Therefore, we searched for shared T-cell clones between the blood sample and the liver biopsy. Interestingly, of the 47 top 1% T-cell clones of the liver, we found 13 shared T-cell clones within the blood sample (**Supplementary Table 12**). To further determine whether shared clones could represent SARS-CoV-2 spike-protein specific T cells, we analyzed a patient (VILI_F) recently published in a case report, who was found to have a $CD8^+$ T cell response against a pre-described Spike-protein epitope ($S_{378-386}$) of SARS-CoV-2.[9] However, the number of sorted $S_{378-386}$ tetramer positive cells from PBMCs, which represent only a fraction of the whole anti-Spike T cell response, was insufficient for following TCR sequencing. However, we were able to perform TCR sequencing from the $S_{378-386}$-depleted fraction. Interestingly, all of the top 1% T-cell clones (n=10) and 96% (n = 47) of the top 50 most frequent T-

cell clones in the liver could be detected in PBMC-sorted spike-protein negative T-cell clones (**Supplementary Table 13**). Yet, none of the shared T-cell clones between liver and blood of these two patients matched to the TCR database described above. Finally, we looked at TCR convergence which was suggested as an indicator of antigen-specific T cell response.[31] Although we observed a higher convergence in VILI samples, it did not reach significance (mean VILI vs. AIH: 2.8% vs. 1.4%; p=0.1248; **Figure 3F**).

In conclusion, our data indicate that COVID-19 vaccination leads to the expansion of a unique set of T cells in the liver, many of which can also be detected in the blood.

Immune Repertoires of VILI and AIH samples have an identical CDR3 length distribution but show variations in TCR beta variable-joining (TRBV-J) and IgH variable-joining (IgHV-J) gene usage

The diversity of CDR3 length is one of the critical determinants of the antigen recognition process by T and B cells. Therefore, we compared CDR3 length distribution in both cohorts. VILI and AIH showed a similar CDR3 length distribution pattern with comparable mean CDR3 nucleotide length in both TCR repertoires (36.72 vs. 36.42; **Figure 4A**) and BCR repertoires (45.78 vs. 46.76; **Figure 4B**). We next evaluated the variable and joining (V-J) region usage in TCR and BCR repertoires of VILI and AIH samples. As shown in **Figure 4C**, T and B cell clones from different patients of the same cohort had a distinct pattern of TRB and IgH V-J usage and each sample had a different set of V-J genes, which was overrepresented or underrepresented. Previously, it was reported that TRBV6-1 and TRBV6-4 were used

less frequently in AIH patients compared to normal controls.[32] Accordingly, we observed that TRBV6-1 and TRBV6-4 genes were used less frequently in the AIH cohort compared to the VILI cohort; however, only TRBV6-1 was statistically significant (**Figure 4D**). Besides, TRBV5-1 was significantly less and TRBV7-6 was significantly more frequently used in VILI in comparison to the AIH cohort (**Figure 4D**). Only one gene from the IgH repertoire, IGHV1-24, displayed a significant usage difference and was found less frequently in the VILI cohort (**Figure 4E**).

DISCUSSION

A growing body of evidence points towards a direct causality between COVID-19 vaccination and hepatitis in very rare cases (summarized in **Supplementary Table 14**).[7-9] The clinical, biochemical, histologic and partially serologic appearance of COVID-19 vaccine-induced hepatitis is similar to AIH.[10, 11] However, it is unclear how these two diseases are related to each other. In addition, the pathophysiological mechanisms of COVID-19 vaccine-induced hepatitis are poorly understood, which prompted us to conduct this comparative study between VILI and AIH. All VILI patients in our study showed a close temporal correlation between COVID-19 vaccination and hepatitis in absence of other causes of acute liver injury. Although two patients were taking drugs potentially associated with liver injury (statin and lercanidipine/telmisartan), a causal relationship is unlikely, because these drugs usually cause liver toxicity within the first few weeks of use and our patients have been taking them for many years without previous adverse effects. Four of the six VILI patients were ANA- and/or AAA- positive, including one with atypical AMA.[6] In addition, serum IgG levels were elevated in two patients. 60% of our patients were classified as probable/definite AIH, according to the simplified criteria, which is only slightly lower than in previously published cohorts of VILI.[15] In contrast, all AIH patients in our cohort had either ANA or ASMA and were all classified as probable/definite AIH according to the simplified criteria. Importantly, all VILI patients responded well to steroid therapy and remained in remission to date.

H&E morphology was very similar between VILI and AIH. A significant difference was found only in confluent necrosis, which was more extensive in VILI. Similarly, a previous report revealed a higher zone 3 necrosis in DI-AILH compared to

AIH.[33] Interestingly, we found no difference between the two groups for eosinophilic infiltrates, a finding often associated with drug-induced liver injury.[33, 34] Whole transcriptome analysis confirmed the close relationship between VILI and AIH. However, GSEA also revealed an overrepresentation of mitochondrial metabolism and oxidative stress-related pathways in VILI compared to AIH. These pathways have been mapped to hepatocytes and are important in DILI[27, 28] and may indicate immunopathological similarities between VILI and DI-AILH. In contrast, we found an increase in pathways related to interferon-gamma signaling in AIH compared to VILI. Indeed, it is well known that interferon pathways are activated in AIH.[35, 36] Interestingly, this interferon response still appears to be significantly higher in AIH than in VILI, although mRNA-based vaccination can also elicit interferon signaling.[37] Furthermore, VILI and AIH were clearly separated from patients with chronic HCV infection or ASH. However, this may be partly explained by the fact, that patients with chronic HCV and ASH in our cohort had cirrhosis, which was not present in VILI and AIH.

Cellular analysis of liver inflammation by transcriptome analysis and multiplex immunofluorescence further showed that VILI was dominated by $CD8^+$ effector T cells, whereas $CD4^+$ effector T cells and B/plasma cells were more prominent in AIH. This is in line with earlier reports showing that activated cytotoxic $CD8^+$ T cells were highly enriched in the liver of patients with VILI.[9] Interestingly, we observed a similar dominance of $CD8^+$ effector T cells in DI-AILH, suggesting that VILI and DI-AILH are closely related and distinct from AIH.

TCR and BCR analysis revealed similar clone numbers and Shannon diversity between VILI and AIH. Yet, we found that VILI had lower evenness in TCR and BCR repertoire, indicating that VILI has expanded clones in T and B cell architecture compared to AIH. Therefore, vaccination induces a more restricted repertoire, as

indicated by the increase of T cell clones in the top 1% of VILI. Additionally, we compared T-cell clones from the liver biopsy of two VILI patients with matched blood samples. Interestingly, many of the high frequency T-cell clones in the liver were also found in the blood of the same patient. However, none of these shared clones matched to spike SARS-CoV-2 in a TCR database. Moreover, we observed a clonal overlap in the patient in whom $CD8^+$ T cells specific for a spike protein epitope ($S_{378-386}$) were depleted from PBMC.[9] Therefore, our data suggest that T-cell clones that do not target a vaccine antigen may be involved in the pathogenesis of VILI. However, we cannot determine whether these high frequency T cells are activated in the liver and then spill over into the periphery or whether T cells from the periphery home to the liver to cause hepatitis.

Interestingly, in our gene usage analysis, we found a decrease in the rearranged TRBV6-1 and TRBV6-4 genes in AIH, in contrast to VILI. This is in line with earlier analysis of AIH, where also a decrease of TRBV6-1 and TRBV6-4 genes has been described.[32] The preferential usage of TRBV6 and TRBV20 family gene variants is a key feature of different subsets of MAIT (mucosal associated invariant T) cells.[38, 39] Loss of MAIT cell subsets in the peripheral blood has been reported in a variety of autoimmune diseases and may be a characteristic for AIH. Furthermore, we observed a decrease in IGHV1-24 in VILI compared to AIH. In contrast, previous studies observed an enrichment of IGHV1-24 in B-cell repertoires[40, 41] after SARS-CoV-2 infection. However, no enrichment in IGHV1-24 was observed in IgH repertoires of healthy individuals after SARS-CoV-2 vaccination.[42]

COVID-19 vaccination is the most effective measure to prevent spreading and reduce mortality after SARS-CoV-2 infection. Moreover, the risk of liver injury during COVID-19 disease by far outweighs the risk of liver injury after vaccination.[43]

Therefore, we strongly advocate vaccination during the pandemic. However, we need to be cautious of hepatitis as a side effect of vaccination and understand VILI better. We are aware of the rather small sample size of our study. However, besides some similarities between VILI and AIH, we found distinct differences between the two entities. TCR beta variable-joining gene usage showed that TRBV6-1 and TRBV6-4 were reduced only in the AIH cohort, which has been described as typical for AIH.[32] Immune infiltration in VILI was also dominated by $CD8^+$ effector T cells, whereas $CD4^+$ effector T cells and $CD79a^+$ B and plasma cells were prominent in AIH. Mitochondrial metabolism and oxidative stress-related pathways were further upregulated in the VILI cohort, in parallel with a more pronounced centrilobular necrosis. Although we can't exclude that some VILI represent activation of latent AIH, our results suggest that in many individuals, VILI represents a separate disease entity, which is distinct from AIH, but more closely related to DI-AILH. Therefore, there is a good chance that many patients with VILI will recover completely and not develop long-term AIH.

LIST OF ABBREVIATIONS

AAA: Anti-actin antibodies

AIH: Autoimmune hepatitis

ALP: Alkaline phosphatase

ALT: Alanine aminotransferase

AMA: Anti-mitochondrial antibody

ANA: Anti-nuclear antibody

ANCA: Anti-neutrophil cytoplasm antibodies

Anti-LC1: Anti-liver cytosol type 1

Anti-LKM: Anti-liver-kidney microsome

Anti-SLA: Anti-soluble liver antigen

ASMA: Anti-smooth muscle antibody

ASH: Alcoholic steatohepatitis

AST: Aspartate aminotransferase

BCR: B-cell receptor

CDR3: Complementarity-determining region 3

CODEX: CO-Detection by IndEXing

COVID-19: Coronavirus disease 2019

DI-AILH: Drug-induced autoimmune-like hepatitis

FFPE: Formalin-fixed and paraffin-embedded

GGT: Gamma-glutamyltransferase

HCV: Hepatitis C virus

H&E: Hematoxylin and eosin

IgH: Immunoglobulin heavy chain

IgHV-J: Immunoglobulin heavy chain variable-joining

MAIT: Mucosal associated invariant T

SARS-CoV-2: Severe acute respiratory syndrome coronavirus 2

TCR: T-cell receptor

TRBV-J: T-cell receptor beta variable-joining

ULN: Upper limit of normal

VILI: Vaccine Induced Liver Injury

ACKNOWLEDGEMENTS

We would like to thank Jan Schneeberger for excellent technical assistance. We thank Dr. Stéphanie Tissot and Dr. Jonathan Thevenet from the Immune Landscape Laboratory of University Hospital of Lausanne for their support in GeoMx experiment and spatial transcriptome sequencing.

REFERENCES

1. https://covid19.who.int/ WHOWCDC-DJAf.
2. **Li M.**, **Wang H.**, **Tian L.**, **Pang Z.**, Yang Q., Huang T., et al. COVID-19 vaccine development: milestones, lessons and prospects. Signal Transduct Target Ther 2022;7:146.
3. **Bril F.**, Al Diffalha S., Dean M., Fettig D.M. Autoimmune hepatitis developing after coronavirus disease 2019 (COVID-19) vaccine: Causality or casualty? J Hepatol 2021;75:222-224.
4. **Rocco A.**, Sgamato C., Compare D., Nardone G. Autoimmune hepatitis following SARS-CoV-2 vaccine: May not be a casuality. J Hepatol 2021;75:728-729.
5. **Londono M.C.**, Gratacos-Gines J., Saez-Penataro J. Another case of autoimmune hepatitis after SARS-CoV-2 vaccination - still casualty? J Hepatol 2021;75:1248-1249.
6. **Ghielmetti M.**, Schaufelberger H.D., Mieli-Vergani G., Cerny A., Dayer E., Vergani D., et al. Acute autoimmune-like hepatitis with atypical anti-mitochondrial antibody after mRNA COVID-19 vaccination: A novel clinical entity? J Autoimmun 2021;123:102706.
7. **Zin Tun G.S.**, Gleeson D., Al-Joudeh A., Dube A., Immune-mediated hepatitis with the Moderna vaccine, no longer a coincidence but confirmed. J Hepatol 2022;76:747-749.
8. **Garrido I.**, Lopes S., Simoes M.S., Rodrigo L., Lopes J., Carneiro F., et al. Autoimmune hepatitis after COVID-19 vaccine - more than a coincidence. J Autoimmun 2021;125:102741.
9. **Boettler T.**, **Csernalabics B.**, Salie H., Luxenburger H., Wischer L., Alizei E.S., et al. SARS-CoV-2 vaccination can elicit a CD8 T-cell dominant hepatitis. J Hepatol 2022;77:653-659.
10. **Codoni G.**, Kirchner T., Engel B., Villamil A.M., Efe C., Stättermayer A.F., et al. Histological and serological features of acute liver injury after SARS-CoV-2 vaccination. JHEP Rep 2023;5:100605.
11. **Efe C.**, Kulkarni A.V., Terziroli Beretta-Piccoli B., Magro B., Stättermayer A., Cengiz M., et al. Liver injury after SARS-CoV-2 vaccination: Features of immune-mediated hepatitis, role of corticosteroid therapy and outcome. Hepatology 2022;76:1576-1586.
12. **Kanduc D.**, Shoenfeld Y. Molecular mimicry between SARS-CoV-2 spike glycoprotein and mammalian proteomes: implications for the vaccine. Immunol Res 2020;68:310-313.
13. **Vojdani A.**, Kharrazian D. Potential antigenic cross-reactivity between SARS-CoV-2 and human tissue with a possible link to an increase in autoimmune diseases. Clin Immunol 2020;217:108480.

14. **Avci E.**, Abasiyanik F. Autoimmune hepatitis after SARS-CoV-2 vaccine: New-onset or flare-up? J Autoimmun 2021;125:102745.
15. **Roy A.**, Verma N., Singh S., Pradhan P., Taneja S., Singh M. Immune-mediated liver injury following COVID-19 vaccination: A systematic review. Hepatol Commun 2022.
16. **Manns M.P.**, Czaja A.J., Gorham J.D., Krawitt E.L., Mieli-Vergani G., Vergani D., et al. Diagnosis and management of autoimmune hepatitis. Hepatology 2010;51:2193-213.
17. **Hennes E.M.**, Zeniya M., Czaja A.J., Dalekos G.N., Krawitt E.L., Bittencourt P.L., et al. Simplified criteria for the diagnosis of autoimmune hepatitis. Hepatology 2008;48:169-76.
18. **Bjornsson E.S.**, Medina-Caliz I., Andrade R.J., Lucerna M.I. Setting up criteria for drug-induced autoimmune-like hepatitis through a systematic analysis of published reports. Hepatol Commun 2022.
19. **Fimiano F.**, D'Amato D., Gambella A., Marzano A., Saracco G.M., Morgando A. Autoimmune hepatitis or drug-induced autoimmune hepatitis following Covid-19 vaccination? Liver Int 2022;42:1204-1205.
20. **Chen Y.**, Xu Z., Wang P., Li X., Shuai Z., Ye D., et al. New-onset autoimmune phenomena post-COVID-19 vaccination. Immunology 2022;165:386-401.
21. **Fontana R.J.**, Seeff L.B., Andrade R.J., Björnsson E., Day C.P.,Serrano J., et al. Standardization of nomenclature and causality assessment in drug-induced liver injury: summary of a clinical research workshop. Hepatology 2010;52:730-42.
22. **Tiniakos D.G.**, Brain J.G., Bury Y.A. Role of Histopathology in Autoimmune Hepatitis. Dig Dis 2015;33 Suppl 2:53-64.
23. **Lohse A.W.**, Sebode M., Bhathal P.S., Clouston A.D., Dienes H.P., Jain D., et al. Consensus recommendations for histological criteria of autoimmune hepatitis from the International AIH Pathology Group: Results of a workshop on AIH histology hosted by the European Reference Network on Hepatological Diseases and the European Society of Pathology: Results of a workshop on AIH histology hosted by the European Reference Network on Hepatological Diseases and the European Society of Pathology. Liver Int 2022;42:1058-1069.
24. **Ishak K.**, Baptista A., Bianchi L., Callea F., Groote J.D., Gudat F., et al. Histological grading and staging of chronic hepatitis. J Hepatol 1995;22:696-9.
25. **Hysenaj L.**, Little S., Kulhanek K., Gbenedio O.M., Rodriguez L., Shen A., et al. SARS-CoV-2 infection studies in lung organoids identify TSPAN8 as novel mediator. bioRxiv 2021.
26. **Pollaci G**, Gorla G, Potenza A, Carrozzini T., Canavero I., Bersano A., et al. Novel Multifaceted Roles for RNF213 Protein. Int J Mol Sci 2022;23.

27. **Mihajlovic M.**, Vinken M.. Mitochondria as the Target of Hepatotoxicity and Drug-Induced Liver Injury: Molecular Mechanisms and Detection Methods. Int J Mol Sci 2022;23.
28. **Yuan L.**, Kaplowitz N. Mechanisms of drug-induced liver injury. Clin Liver Dis 2013;17:507-18, vii.
29. **Aran D.**, Hu Z., Butte A.J. xCell: digitally portraying the tissue cellular heterogeneity landscape. Genome Biol 2017;18:220.
30. **Black S.**, **Phillips D.**, **Hickey J.W.**, Kennedy-Darling J., Venkataraaman V.G., Samusik N., et al. CODEX multiplexed tissue imaging with DNA-conjugated antibodies. Nat Protoc 2021;16:3802-3835.
31. **Pan M.Y.**, Li B. T cell receptor convergence is an indicator of antigen-specific T cell response in cancer immunotherapies. https://www.biorxiv.org/content/10.1101/2022.06.15.495325v3 2022.
32. **Schultheiss C.**, Simnica D., Willscher E., Oberle A., Fanchi L., Bonzanni N., et al. Next-Generation Immunosequencing Reveals Pathological T-Cell Architecture in Autoimmune Hepatitis. Hepatology 2021;73:1436-1448.
33. **Qu L.M.**, Wang S.H. Yang K., Brigstock D.R., Sun L., Gao R. et al. CD4(+)Foxp3(+)CD25(+/-) Tregs characterize liver tissue specimens of patients suffering from drug-induced autoimmune hepatitis: A clinical-pathological study. Hepatobiliary Pancreat Dis Int 2018;17:133-139.
34. **Suzuki A.**, Brunt E.M., Kleiner D.E., Miquel R., Smyrk T.C., Andrade R.J., et al. The use of liver biopsy evaluation in discrimination of idiopathic autoimmune hepatitis versus drug-induced liver injury. Hepatology 2011;54:931-9.
35. **Terziroli Beretta-Piccoli B.**, Mieli-Vergani G., Vergani D. Autoimmmune hepatitis. Cell Mol Immunol 2022;19:158-176.
36. **Liberal R.**, de Boer Y.S., Heneghan M.A. Established and novel therapeutic options for autoimmune hepatitis. Lancet Gastroenterol Hepatol 2021;6:315-326.
37. **Arunachalam P.S.**, **Scott M.K.D.**, **Hagan T.**, Li C., Feng Y., Wimmers F., et al. Systems vaccinology of the BNT162b2 mRNA vaccine in humans. Nature 2021;596:410-416.
38. **Reantragoon R.**, **Corbett A.J.**, Sakala I.G., Gherardin N.A., Furness J.B., Chen Z., et al. Antigen-loaded MR1 tetramers define T cell receptor heterogeneity in mucosal-associated invariant T cells. J Exp Med 2013;210:2305-20.
39. **Lepore M.**, Kalinichenko A., Colone A., Paleja B., Singhal A., Tschumi A., et al. Parallel T-cell cloning and deep sequencing of human MAIT cells reveal stable oligoclonal TCRbeta repertoire. Nat Commun 2014;5:3866.

40. **Voss W.N.**, Hou Y.J., Johnson N.V., Delidakis G., Kim J.E., Javanmardi K., et al. Prevalent, protective, and convergent IgG recognition of SARS-CoV-2 non-RBD spike epitopes. Science 2021;372:1108-1112.

41. **Nielsen S.C.A.**, Yang F., Jackson K.J.L., Ramona A.H., Röltgen K., Jean G.H., et al. Human B Cell Clonal Expansion and Convergent Antibody Responses to SARS-CoV-2. Cell Host Microbe 2020;28:516-525 e5.

42. **Kotagiri P.**, Mescia F., Rae W.M., Bergamaschi L., Tuong Z.K., Turner L., et al. B cell receptor repertoire kinetics after SARS-CoV-2 infection and vaccination. Cell Rep 2022;38:110393.

43. **Wong C.K.H.**, **Mak L.Y.**, Au I.C.H., Lai F.T.T., Li X., Wan E.Y.F.W., et al. Risk of acute liver injury following the mRNA (BNT162b2) and inactivated (CoronaVac) COVID-19 vaccines. J Hepatol 2022;77:1339-1348.

TABLES

Patient ID	Age	Sex	Symptoms	Symptoms after vacc.	Drugs at time of vaccination	Therapy (Prednisone)*	Follow-up months	Remission
VILI1	48	f	fatigue, abdominal pain	2d after 2nd vaccination	multivitamines	40mg/d for 3 months	18	Yes
VILI2	85	m	nausea, dark urine	5d after 1st vaccination	none	None	18	Yes
VILI3	21	f	fatigue, jaundice, nausea	21d after 2nd vaccination	oral contraceptive	60mg/d for 3 months	15	Yes
VILI4	53	m	fatigue, jaundice, nausea	7d after 2nd vaccination	none	40mg/d for 3 months	18	Yes
VILI5	63	m	fatigue, jaundice, weight loss	10d after 1st vaccination	aspirin, rosuvastatin, metformin	40mg/d for 11months	18	Yes
VILI6	78	m	none	28d after 1st vaccination#	lercanidipine, telmisartan	40mg/d for 5 months	12	Yes

Table 1. Cohort of patients with liver injury after COVID-19 vaccination.

Abbreviations: d: days, f: female, m: male, vacc.: vaccination, *Initial dose, reduced thereafter according to liver enzyme levels and/or clinical course, #only elevated liver enzymes

FIGURE LEGENDS

Figure 1. Whole transcriptome analysis reveals distinct differences between VILI and AIH. (A) Principal component analysis of VILI (n=6), AIH (n=9), ASH (n=17), HCV hepatitis (n=13) and normal liver (n=3). **(B)** Volcano plot for differentially expressed genes between VILI and AIH cohort. Genes with a $\log_2$ fold change>0.58 and p_{adj}<0.05 were accepted as differentially expressed between cohorts. **(C)** qPCR result of *TSPAN8* and *RNF213* expression. VILI cohort, n=6; AIH cohort, n=5; normal liver, n=3. **(D)** Unsupervised hierarchical clustering with differentially expressed genes between VILI and AIH samples. Arrows show the two genes which underwent validation of gene expression by qPCR. **(E)** Gene set enrichment analysis of VILI and AIH cohorts. Only pathways with p_{adj}<0.05 are shown.

Figure 2. Immunophenotyping of VILI and AIH with xCell method and multiplex immunofluorescence. **(A)** *In silico* immunophenotyping of VILI and AIH cases with xCell method. **(B)** Portal and centrilobular immune cell densities were quantified with CODEX multiplex immunofluorescence. CV: central vein; PV: portal vein. **(C)** Immune cell distribution in the portal and centrilobular region of VILI and AIH samples. Bar graphs indicate mean and standard error of mean (SEM) of immune cell densities (cells/mm^2). **(D)** $CD3^+$ $CD8^+$ and $CD3^+$ $CD4^+$ $FoxP3^-$ cell density in the portal and centrilobular region of VILI and AIH samples. **(E)** Ratio of $CD3^+$ $CD8^+$/$CD3^+$ $CD4^+$ T cells in the portal region of VILI and AIH cohorts. **(F)** $CD3^+$ $CD4^+$ $FoxP3^+$ cell density in the portal and centrilobular region of VILI and AIH samples. **(G)** $CD20^+$ and $CD79a^+$ cell density in the portal and centrilobular region of VILI and AIH samples. **(H)** Ratio of $CD3^+$ $CD8^+$/$CD79a^+$ T cells in the portal region of VILI and AIH cohorts. **(I)** Correlation

analysis between Ishak grading and portal total T cell ($CD3^+$) and B-cell ($CD79a^+$) density. The black line shows the linear regression line and dotted lines represent the 95% confidence interval upper and lower limits. Each dot represents a patient. * $p<0.05$, ** $p<0.01$ (two-group comparison: wilcoxon rank-sum test, correlation analysis: Spearman rank correlation test).

Figure 3. Global immune metrics and clonal space analysis of TCR and BCR repertoires of VILI and AIH. (A) Global TCR repertoire metrics (clone number, Shannon diversity, evenness) of VILI (n=6) and AIH (n=6) patients. **(B)** Global BCR repertoire metrics (clone number, Shannon diversity, evenness) of VILI (n=6) and AIH (n=9) cohorts. **(C)** Clonal space occupied by T-cell clones according to their frequency ranking. **(D)** Correlation of top 1% ranked total TCR frequency and evenness of VILI and AIH TCR repertoires. The black line shows the linear regression line and dotted lines represent the 95% confidence interval upper and lower limits. **(E)** Clonal space occupied by B cell clones according to their frequency ranking. **(F)** TCR convergence of VILI and AIH cohorts. Each dot represents a patient. * $p<0.05$, ** $p<0.01$, *** $p<0.001$ (two-group comparison: unpaired student *t* test, correlation analysis: Spearman rank correlation test). ns: not significant.

Figure 4. Identical CDR3 length distribution but variations in TRBV-J and IgHV-J gene usage between VILI and AIH patients. (A) CDR3 nucleotide length distribution of TCR repertoires of VILI and AIH patients. **(B)** CDR3 nucleotide length distribution of BCR repertoires of VILI and AIH samples. **(C)** Heatmap of TCR-β chain and BCR CDR3 region variable and joining gene usage proportion in each sample. **(D)** Preferential usage of TRBV6-1, TRBV6-4, TRBV5-1, and TRBV7-6. **(E)** Preferential usage of IGHV1-24 in AIH patients. For TCR analysis 6 VILI and 6 AIH patients, for BCR analysis 6 VILI and 9 AIH patients were included. Each dot represents a patient. * $p<0.05$, ** $p<0.01$, *** $p<0.001$ (two-group comparison: wilcoxon rank-sum test). ns: not significant.

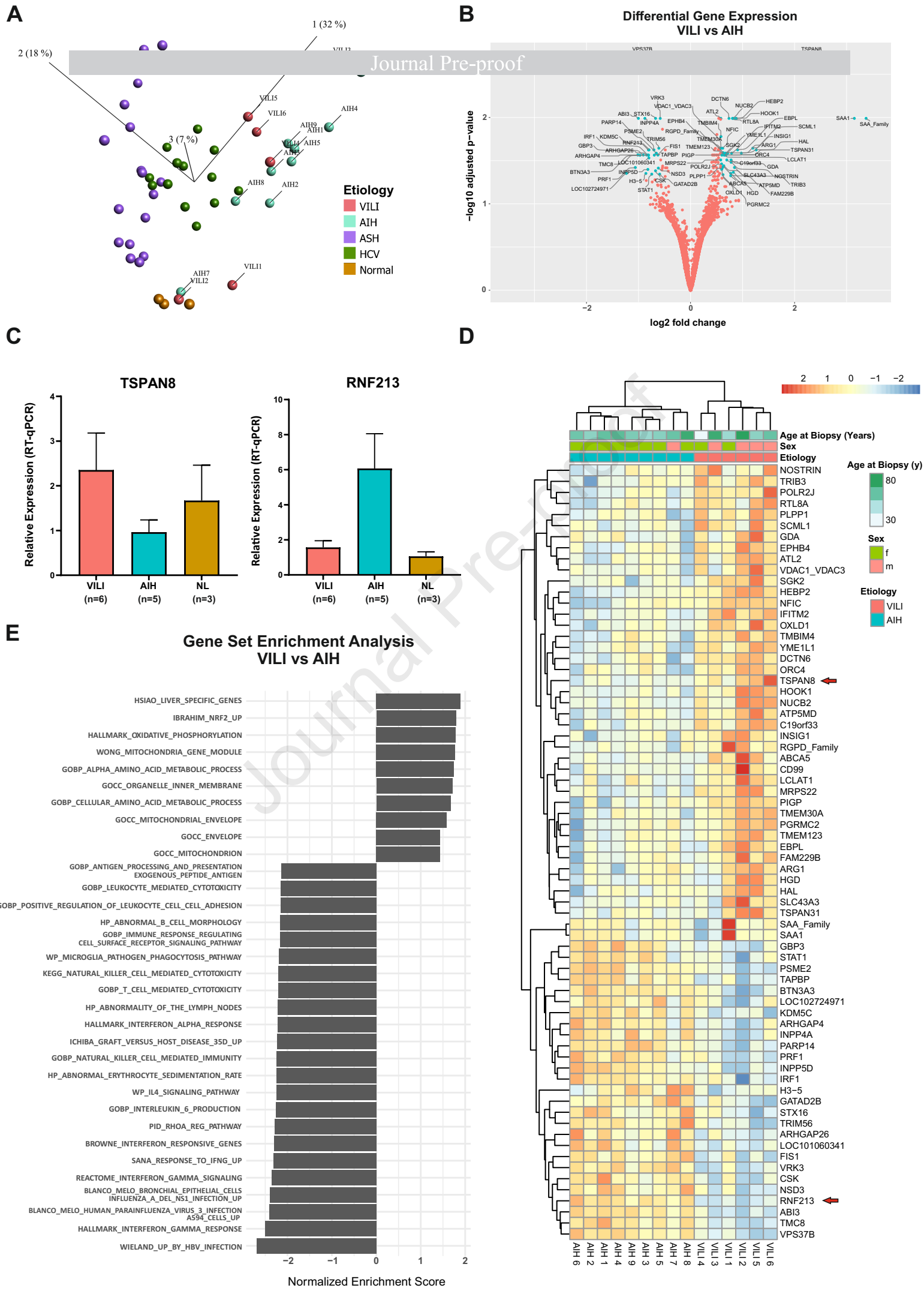

FIGURE 1

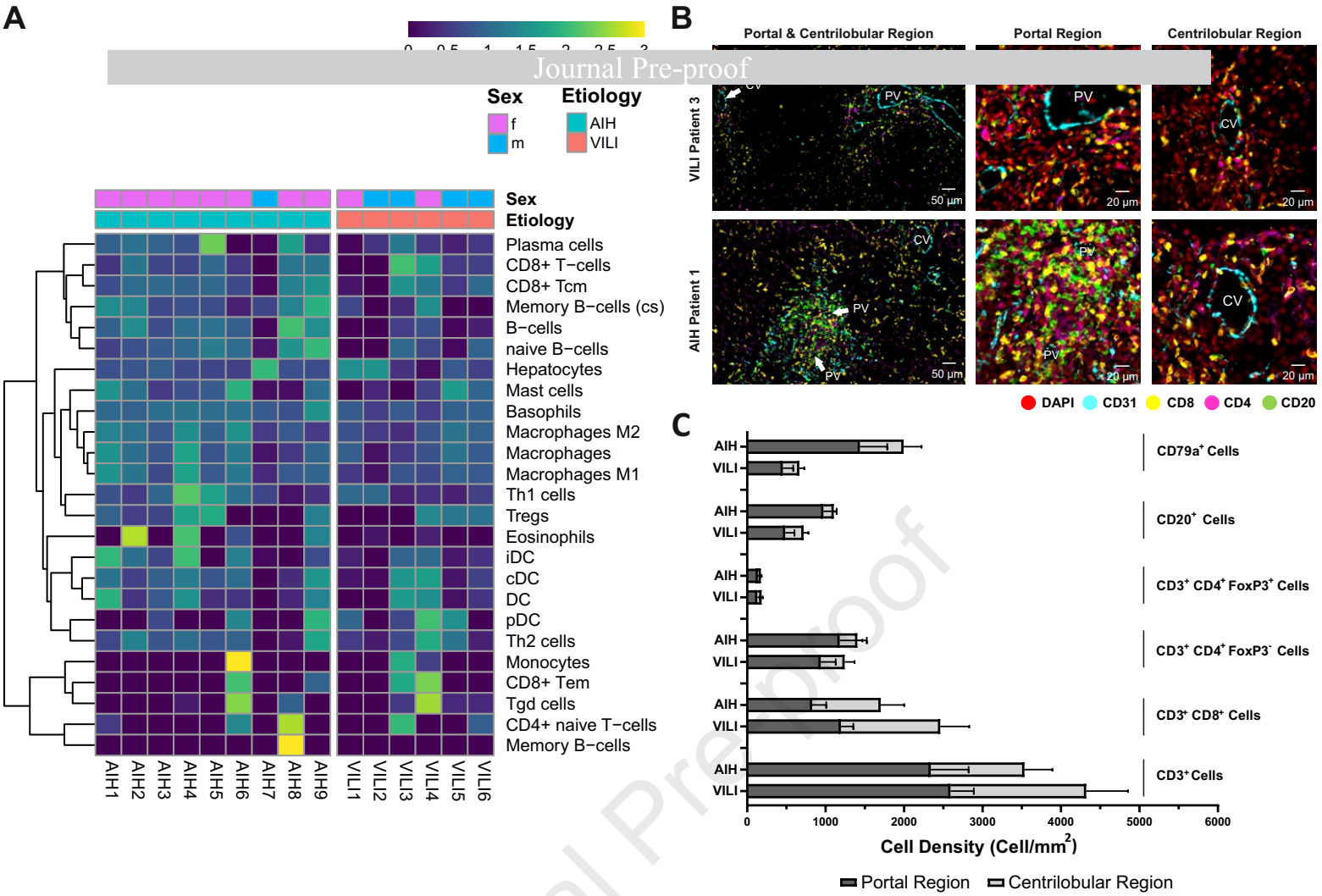

FIGURE 2

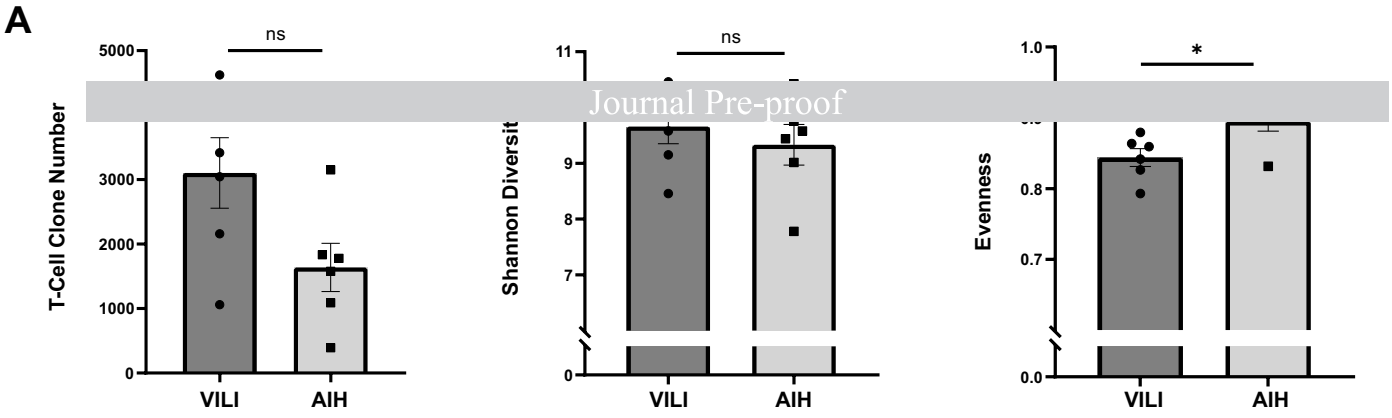

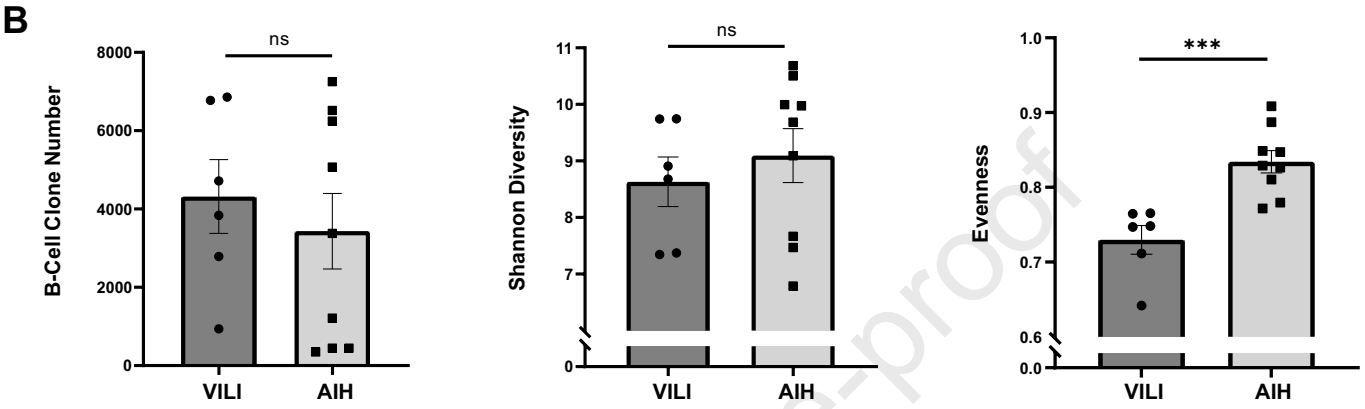

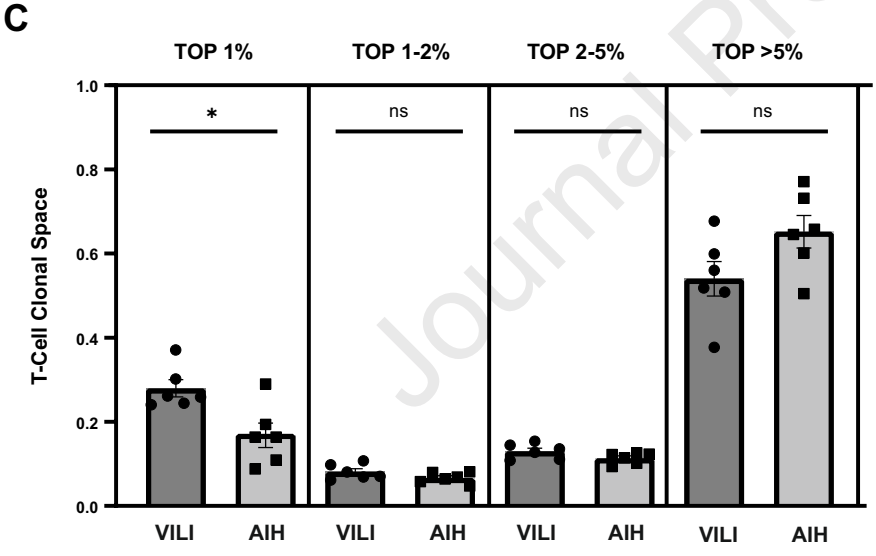

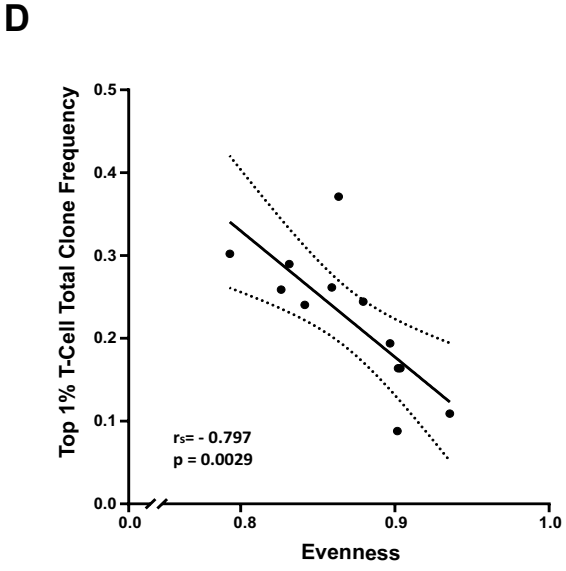

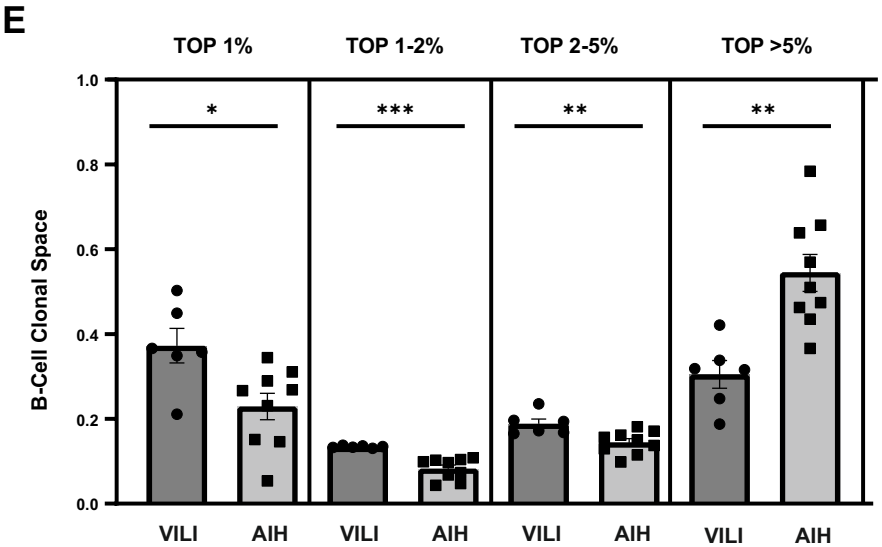

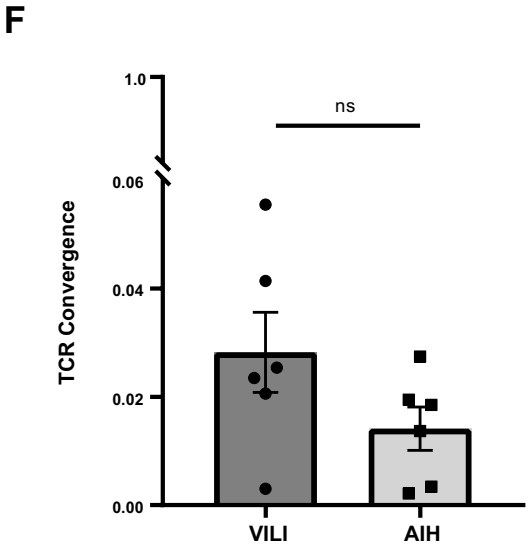

FIGURE 3

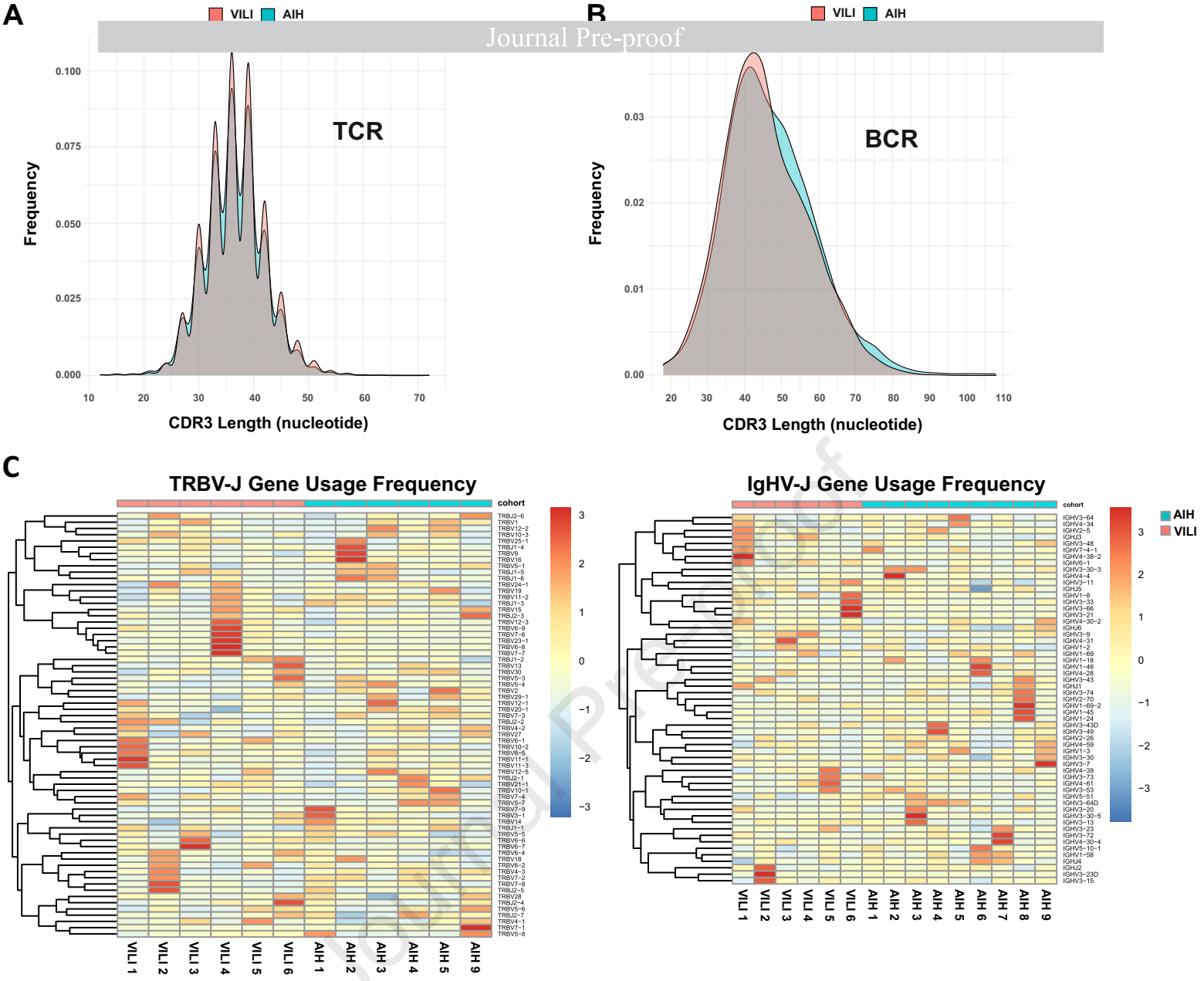

FIGURE 4

HIGHLIGHTS

VILI demonstrates similarities to AIH but also distinct differences

VILI shows enrichment in mitochondrial metabolism and oxidative stress-related pathways

VILI is dominated by $CD8^+$ T cell infiltrates

VILI presents oligoclonal immune response and distinct TCR beta chain usage